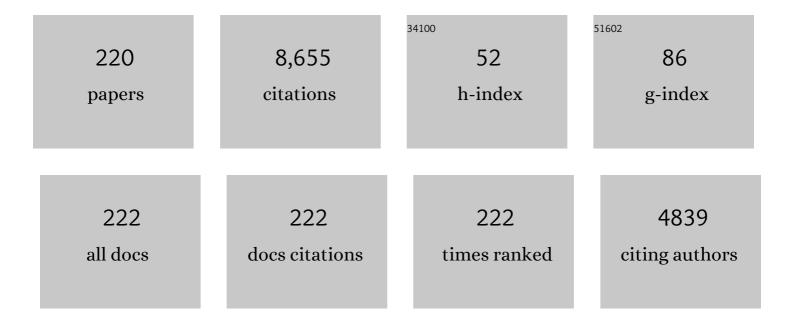
Alejandro Pérez-RodrÃ-guez

List of Publications by Year in descending order

Source: https://exaly.com/author-pdf/4083402/publications.pdf

Version: 2024-02-01



#	Article	IF	CITATIONS
1	Evaluation of defect formation in chalcopyrite compounds under Cu-poor conditions by advanced structural and vibrational analyses. Acta Materialia, 2022, 223, 117507.	7.9	5
2	Ultrathin Wideâ€Bandgap aâ€Si:Hâ€Based Solar Cells for Transparent Photovoltaic Applications. Solar Rrl, 2022, 6, 2100909.	5.8	7
3	Insights into the Effects of RbFâ€Postâ€Deposition Treatments on the Absorber Surface of High Efficiency Cu(In,Ga)Se ₂ Solar Cells and Development of Analytical and Machine Learning Process Monitoring Methodologies Based on Combinatorial Analysis. Advanced Energy Materials, 2022, 12, .	19.5	6
4	Characterization of the Stability of Indium Tin Oxide and Functional Layers for Semitransparent Backâ€Contact Applications on Cu(in,Ga)Se ₂ Solar Cells. Solar Rrl, 2022, 6, .	5.8	8
5	Kinetics and phase analysis of kesterite compounds: Influence of chalcogen availability in the reaction pathway. Materialia, 2022, 24, 101509.	2.7	2
6	Defect depth-profiling in kesterite absorber by means of chemical etching and surface analysis. Applied Surface Science, 2021, 540, 148342.	6.1	6
7	Rear interface engineering of kesterite Cu ₂ ZnSnSe ₄ solar cells by adding CuGaSe ₂ thin layers. Progress in Photovoltaics: Research and Applications, 2021, 29, 334-343.	8.1	11
8	Combinatorial and machine learning approaches for the analysis of Cu ₂ ZnGeSe ₄ : influence of the off-stoichiometry on defect formation and solar cell performance. Journal of Materials Chemistry A, 2021, 9, 10466-10476.	10.3	13
9	Effective module level encapsulation of CIGS solar cells with Al2O3 thin film grown by atomic layer deposition. Solar Energy Materials and Solar Cells, 2021, 222, 110914.	6.2	8
10	Bromine etching of kesterite thin films: perspectives in depth defect profiling and device performance improvement. , 2021, , .		1
11	Insights on the Thermal Stability of the Sb ₂ Se ₃ Quasiâ€1D Photovoltaic Technology. Solar Rrl, 2021, 5, 2100517.	5.8	2
12	Insights into interface and bulk defects in a high efficiency kesterite-based device. Energy and Environmental Science, 2021, 14, 507-523.	30.8	48
13	spectrapepper: A Python toolbox for advanced analysis of spectroscopic data for materials and devices Journal of Open Source Software, 2021, 6, 3781.	4.6	2
14	Point defects, compositional fluctuations, and secondary phases in non-stoichiometric kesterites. JPhys Energy, 2020, 2, 012002.	5.3	92
15	Structural and vibrational properties of α- and π-SnS polymorphs for photovoltaic applications. Acta Materialia, 2020, 183, 1-10.	7.9	43
16	Vibrational Properties of RbInSe ₂ : Raman Scattering Spectroscopy and First-Principle Calculations. Journal of Physical Chemistry C, 2020, 124, 1285-1291.	3.1	5
17	UVâ€Selective Optically Transparent Zn(O,S)â€Based Solar Cells. Solar Rrl, 2020, 4, 2070112.	5.8	0
18	Rear Band gap Grading Strategies on Sn–Ge-Alloyed Kesterite Solar Cells. ACS Applied Energy Materials. 2020. 3. 10362-10375.	5.1	29

#	Article	IF	CITATIONS
19	UV‧elective Optically Transparent Zn(O,S)â€Based Solar Cells. Solar Rrl, 2020, 4, 2000470.	5.8	12
20	Cu-Sn-S system: Vibrational properties and coexistence of the Cu2SnS3, Cu3SnS4 and Cu4SnS4 compounds. Scripta Materialia, 2020, 186, 180-184.	5.2	15
21	Transition-Metal Oxides for Kesterite Solar Cells Developed on Transparent Substrates. ACS Applied Materials & Interfaces, 2020, 12, 33656-33669.	8.0	29
22	Efficient Seâ€Rich Sb ₂ Se ₃ /CdS Planar Heterojunction Solar Cells by Sequential Processing: Control and Influence of Se Content. Solar Rrl, 2020, 4, 2070075.	5.8	5
23	Efficient Seâ€Rich Sb ₂ Se ₃ /CdS Planar Heterojunction Solar Cells by Sequential Processing: Control and Influence of Se Content. Solar Rrl, 2020, 4, 2000141.	5.8	23
24	Over 10% Efficient Wide Bandgap CIGSe Solar Cells on Transparent Substrate with Na Predeposition Treatment. Solar Rrl, 2020, 4, 2000284.	5.8	8
25	Multiwavelength excitation Raman scattering study of Sb ₂ Se ₃ compound: fundamental vibrational properties and secondary phases detection. 2D Materials, 2019, 6, 045054.	4.4	69
26	Study and optimization of alternative MBEâ€deposited metallic precursors for highly efficient kesterite CZTSe:Ge solar cells. Progress in Photovoltaics: Research and Applications, 2019, 27, 779-788.	8.1	12
27	CuZnInSe ₃ â€based solar cells: Impact of copper concentration on vibrational and structural properties and device performance. Progress in Photovoltaics: Research and Applications, 2019, 27, 716-723.	8.1	7
28	Defect characterisation in Cu ₂ ZnSnSe ₄ kesterites <i>via</i> resonance Raman spectroscopy and the impact on optoelectronic solar cell properties. Journal of Materials Chemistry A, 2019, 7, 13293-13304.	10.3	63
29	Progress and Perspectives of Thin Film Kesterite Photovoltaic Technology: A Critical Review. Advanced Materials, 2019, 31, e1806692.	21.0	333
30	Impact of Thin CuGa Layers Added at the Rear Interface of Cu2ZnSnSe4 Solar Cells. , 2019, , .		0
31	Spectroscopic ellipsometry study of Cu2ZnSnS4 bulk poly-crystals. Applied Physics Letters, 2018, 112, 161901.	3.3	6
32	How small amounts of Ge modify the formation pathways and crystallization of kesterites. Energy and Environmental Science, 2018, 11, 582-593.	30.8	169
33	C <scp>ZTS</scp> e solar cells developed on polymer substrates: Effects of lowâ€ŧemperature processing. Progress in Photovoltaics: Research and Applications, 2018, 26, 55-68.	8.1	23
34	Double band gap gradients in sequentially processed photovoltaic absorbers from the Cu(In,Ga)Se ₂ â€ZnSe pseudobinary system. Progress in Photovoltaics: Research and Applications, 2018, 26, 135-144.	8.1	7
35	Enhanced Heteroâ€Junction Quality and Performance of Kesterite Solar Cells by Aluminum Hydroxide Nanolayers and Efficiency Limitation Revealed by Atomicâ€resolution Scanning Transmission Electron Microscopy. Solar Rrl, 2018, 3, 1800279.	5.8	6
36	An in-depth investigation on the grain growth and the formation of secondary phases of ultrasonic-sprayed Cu2ZnSnS4 based thin films assisted by Na crystallization catalyst. Solar Energy, 2018, 176, 277-286.	6.1	8

#	Article	IF	CITATIONS
37	Revealing the beneficial effects of Ge doping on Cu ₂ ZnSnSe ₄ thin film solar cells. Journal of Materials Chemistry A, 2018, 6, 11759-11772.	10.3	46
38	Understanding the cell-to-module efficiency gap in Cu(In,Ga)(S,Se)2 photovoltaics scale-up. Nature Energy, 2018, 3, 466-475.	39.5	76
39	Nondestructive Raman Scattering Assessment of Solution-Processed ZnO-Doped Layers for Photovoltaic Applications. Journal of Physical Chemistry C, 2017, 121, 3212-3218.	3.1	17
40	Structural Polymorphism in "Kesterite―Cu ₂ ZnSnS ₄ : Raman Spectroscopy and First-Principles Calculations Analysis. Inorganic Chemistry, 2017, 56, 3467-3474.	4.0	84
41	Characterization of Cu ₂ SnS ₃ polymorphism and its impact on optoelectronic properties. Journal of Materials Chemistry A, 2017, 5, 23863-23871.	10.3	56
42	Resonant Raman scattering based approaches for the quantitative assessment of nanometric ZnMgO layers in high efficiency chalcogenide solar cells. Scientific Reports, 2017, 7, 1144.	3.3	9
43	Towards In-reduced photovoltaic absorbers: Evaluation of zinc-blende CuInSe2-ZnSe solid solution. Solar Energy Materials and Solar Cells, 2017, 160, 26-33.	6.2	15
44	Special issue "Nanotechnology for next generation high efficiency photovoltaics: NEXTGEN NANOPV Spring International School & Workshop― Solar Energy Materials and Solar Cells, 2016, 158, 123-125.	6.2	0
45	Optical properties of quaternary kesterite-type Cu ₂ Zn(Sn _{1â^'x} Ge _x)S ₄ crystalline alloys: Raman scattering, photoluminescence and first-principle calculations. RSC Advances, 2016, 6, 67756-67763.	3.6	25
46	Post-deposition annealing of Cu <inf>2</inf> ZnSnSe <inf>4</inf> /CdS based solar cells: Analysis of the absorber's surface defects. , 2016, , .		0
47	Enhancing grain growth and boosting Voc in CZTSe absorber layers $\hat{a} \in \mathbb{C}$ Is Ge doping the answer?. , 2016, , .		1
48	The Cu(In, Ga)Se <inf>2</inf> -ZnSe system: Optimizing solid solutions for high V <inf>OC</inf> photovoltaic devices. , 2016, , .		0
49	CdS bi-layers for optimized CdS/Cu <inf>2</inf> ZnSnSe <inf>4</inf> solar cells. , 2016, , .		0
50	Vitreous enamel as sodium source for efficient kesterite solar cells on commercial ceramic tiles. Solar Energy Materials and Solar Cells, 2016, 154, 11-17.	6.2	10
51	<i>V</i> _{oc} Boosting and Grain Growth Enhancing Ge-Doping Strategy for Cu ₂ ZnSnSe ₄ Photovoltaic Absorbers. Journal of Physical Chemistry C, 2016, 120, 9661-9670.	3.1	69
52	Cu ₂ ZnSnSe ₄ -Based Solar Cells With Efficiency Exceeding 10% by Adding a Superficial Ge Nanolayer: The Interaction Between Ge and Na. IEEE Journal of Photovoltaics, 2016, 6, 754-759.	2.5	28
53	Phosphonic acids aid composition adjustment in the synthesis of Cu2+x Zn1â^'x SnSe4â^'y nanoparticles. Journal of Nanoparticle Research, 2016, 18, 1.	1.9	5
54	Influence of Amorphous Silicon Carbide Intermediate Layer in the Back-Contact Structure of Cu ₂ ZnSnSe ₄ Solar Cells. IEEE Journal of Photovoltaics, 2016, 6, 1327-1332.	2.5	8

Alejandro Pérez-RodrÃgue

#	Article	IF	CITATIONS
55	Raman scattering analysis of the surface chemistry of kesterites: Impact of post-deposition annealing and Cu/Zn reordering on solar cell performance. Solar Energy Materials and Solar Cells, 2016, 157, 462-467.	6.2	71
56	Cu ₂ ZnSnSe ₄ solar cells with 10.6% efficiency through innovative absorber engineering with Ge superficial nanolayer. Progress in Photovoltaics: Research and Applications, 2016, 24, 1359-1367.	8.1	77
57	Polarized Raman scattering study of kesterite type Cu2ZnSnS4 single crystals. Scientific Reports, 2016, 6, 19414.	3.3	88
58	Bi-directional crystallization of Cu <inf>2</inf> ZnSnSe <inf>4</inf> assisted with back/front Ge nanolayers. , 2016, , .		1
59	The importance of back contact modification in Cu2ZnSnSe4 solar cells: The role of a thin MoO2 layer. Nano Energy, 2016, 26, 708-721.	16.0	77
60	Optical phonons in the kesterite Cu ₂ ZnGeS ₄ semiconductor: polarized Raman spectroscopy and first-principle calculations. RSC Advances, 2016, 6, 13278-13285.	3.6	35
61	Alkali doping strategies for flexible and light-weight Cu ₂ ZnSnSe ₄ solar cells. Journal of Materials Chemistry A, 2016, 4, 1895-1907.	10.3	88
62	Optical methodology for process monitoring of chalcopyrite photovoltaic technologies: Application to low cost Cu(In,Ca)(S,Se)2 electrodeposition based processes. Solar Energy Materials and Solar Cells, 2016, 158, 168-183.	6.2	51
63	Fermi resonance in the phonon spectra of quaternary chalcogenides of the type Cu ₂ ZnGeS ₄ . Journal of Physics Condensed Matter, 2016, 28, 065401.	1.8	27
64	Optical and electrical properties of In-doped Cu2ZnSnSe4. Solar Energy Materials and Solar Cells, 2016, 151, 44-51.	6.2	19
65	Secondary phase and Cu substitutional defect dynamics in kesterite solar cells: Impact on optoelectronic properties. Solar Energy Materials and Solar Cells, 2016, 149, 304-309.	6.2	82
66	Impact of Na Dynamics at the Cu ₂ ZnSn(S,Se) ₄ /CdS Interface During Post Low Temperature Treatment of Absorbers. ACS Applied Materials & Interfaces, 2016, 8, 5017-5024.	8.0	72
67	Effect of rapid thermal annealing on the Mo back contact properties for Cu2ZnSnSe4 solar cells. Journal of Alloys and Compounds, 2016, 675, 158-162.	5.5	14
68	Towards high performance Cd-free CZTSe solar cells with a ZnS(O,OH) buffer layer: the influence of thiourea concentration on chemical bath deposition. Journal Physics D: Applied Physics, 2016, 49, 125602.	2.8	39
69	Raman scattering quantitative assessment of the anion composition ratio in Zn(O,S) layers for Cd-free chalcogenide-based solar cells. RSC Advances, 2016, 6, 24536-24542.	3.6	13
70	Role of S and Se atoms on the microstructural properties of kesterite Cu ₂ ZnSn(S _x Se _{1â''x}) ₄ thin film solar cells. Physical Chemistry Chemical Physics, 2016, 18, 8692-8700.	2.8	43
71	Wide band-gap tuning Cu2ZnSn1â^'xGexS4 single crystals: Optical and vibrational properties. Solar Energy Materials and Solar Cells, 2016, 158, 147-153.	6.2	44
72	Resonant Raman scattering of ZnS _x Se _{1â^'x} solid solutions: the role of S and Se electronic states. Physical Chemistry Chemical Physics, 2016, 18, 7632-7640.	2.8	43

#	Article	IF	CITATIONS
73	High efficiency Cu2ZnSnSe4:In doped based solar cells. , 2015, , .		1
74	Cu2ZnSnSe4 based solar cells prepared at high temperatures on Si/SiO2 sodium-free substrate. , 2015, , .		0
75	Large Efficiency Improvement in Cu ₂ ZnSnSe ₄ Solar Cells by Introducing a Superficial Ge Nanolayer. Advanced Energy Materials, 2015, 5, 1501070.	19.5	188
76	Solar Cells: Large Efficiency Improvement in Cu2ZnSnSe4Solar Cells by Introducing a Superficial Ge Nanolayer (Adv. Energy Mater. 21/2015). Advanced Energy Materials, 2015, 5, n/a-n/a.	19.5	0
77	Large performance improvement in Cu2ZnSnSe4 based solar cells by surface engineering with a nanometric Ge layer. , 2015, , .		4
78	Optimization of CdS buffer layer for highâ€performance Cu ₂ ZnSnSe ₄ solar cells and the effects of light soaking: elimination of crossover and red kink. Progress in Photovoltaics: Research and Applications, 2015, 23, 1660-1667.	8.1	110
79	Impact of the structure of Mo(S,Se) ₂ interfacial region in electrodeposited Culn(S,Se) ₂ solar cells. Physica Status Solidi (A) Applications and Materials Science, 2015, 212, 61-66.	1.8	8
80	Raman scattering quantitative analysis of the anion chemical composition in kesterite Cu2ZnSn(SxSe1â^²x)4 solid solutions. Journal of Alloys and Compounds, 2015, 628, 464-470.	5.5	69
81	Influence of compositionally induced defects on the vibrational properties of device grade Cu2ZnSnSe4 absorbers for kesterite based solar cells. Applied Physics Letters, 2015, 106, .	3.3	135
82	Non-destructive assessment of ZnO:Al window layers in advanced Cu(In,Ga)Se ₂ photovoltaic technologies. Physica Status Solidi (A) Applications and Materials Science, 2015, 212, 56-60.	1.8	12
83	Advanced characterization of electrodeposition-based high efficiency solar cells: Non-destructive Raman scattering quantitative assessment of the anion chemical composition in Cu(In,Ga)(S,Se)2 absorbers. Solar Energy Materials and Solar Cells, 2015, 143, 212-217.	6.2	26
84	Complex Surface Chemistry of Kesterites: Cu/Zn Reordering after Low Temperature Postdeposition Annealing and Its Role in High Performance Devices. Chemistry of Materials, 2015, 27, 5279-5287.	6.7	99
85	Synthesis of CuIn(S,Se)2 quaternary alloys by screen printing and selenization-sulfurization sequential steps: Development of composition graded absorbers for low cost photovoltaic devices. Materials Chemistry and Physics, 2015, 160, 237-243.	4.0	9
86	Structural characterisation of Cu _{2.04} Zn _{0.91} Sn _{1.05} S _{2.08} Se _{1.92} . Physica Status Solidi C: Current Topics in Solid State Physics, 2015, 12, 588-591.	0.8	19
87	Impact of Cu–Au type domains in high current density CuInS 2 solar cells. Solar Energy Materials and Solar Cells, 2015, 139, 101-107.	6.2	15
88	Formation and impact of secondary phases in Cu-poor Zn-rich Cu2ZnSn(S1â^'Se)4 (0â‰ y â‰⊉) based solar cells. Solar Energy Materials and Solar Cells, 2015, 140, 289-298.	6.2	60
89	Compositional paradigms in multinary compound systems for photovoltaic applications: a case study of kesterites. Journal of Materials Chemistry A, 2015, 3, 9451-9455.	10.3	34
90	Towards the growth of Cu 2 ZnSn 1â^'x Ge x S 4 thin films by a single-stage process: Effect of substrate temperature and composition. Solar Energy Materials and Solar Cells, 2015, 139, 1-9.	6.2	33

#	Article	IF	CITATIONS
91	Multiwavelength excitation Raman scattering analysis of bulk and two-dimensional MoS ₂ : vibrational properties of atomically thin MoS ₂ layers. 2D Materials, 2015, 2, 035006.	4.4	97
92	Zn-poor Cu ₂ ZnSnSe ₄ thin films and solar cell devices. Physica Status Solidi (A) Applications and Materials Science, 2015, 212, 109-115.	1.8	13
93	Synthesis of Cu2ZnSnS4nanoparticles and analysis of secondary phases in powder pellets. Physica Status Solidi (A) Applications and Materials Science, 2015, 212, 329-335.	1.8	8
94	Spray-deposited CuIn _{1â^'<i>x</i>} Ga _{<i>x</i>} Se ₂ solar cell absorbers: Influence of spray deposition parameters and crystallization promoters. Physica Status Solidi (A) Applications and Materials Science, 2015, 212, 67-71.	1.8	7
95	CuIn1â^'Al Se2 thin film solar cells with depth gradient composition prepared by selenization of evaporated metallic precursors. Solar Energy Materials and Solar Cells, 2015, 132, 245-251.	6.2	22
96	Raman scattering analysis of electrodeposited Cu(In,Ga)Se2 solar cells: Impact of ordered vacancy compounds on cell efficiency. Applied Physics Letters, 2014, 105, .	3.3	49
97	Multiwavelength excitation Raman scattering of Cu2ZnSn(SxSe1â^'x)4 (O â‰â€‰ <i>x</i> â‰â€‰1) µ thin films: Vibrational properties of sulfoselenide solid solutions. Applied Physics Letters, 2014, 105, .	oolycrysta	lline 64
98	Rapid thermal processing of Cu <inf>2</inf> ZnSnSe <inf>4</inf> thin films. , 2014, , .		1
99	Simplified formation process for Cu2ZnSnS4-based solar cells. Thin Solid Films, 2014, 573, 148-158.	1.8	15
100	Structural study and Raman scattering analysis of Cu_2ZnSiTe_4 bulk crystals. Optics Express, 2014, 22, A1936.	3.4	11
101	Rapid annealing of reactively sputtered precursors for Cu ₂ ZnSnS ₄ solar cells. Progress in Photovoltaics: Research and Applications, 2014, 22, 10-17.	8.1	131
102	Secondary phase formation in Znâ€rich Cu ₂ ZnSnSe ₄ â€based solar cells annealed in low pressure and temperature conditions. Progress in Photovoltaics: Research and Applications, 2014, 22, 479-487.	8.1	97
103	Spectroscopic ellipsometry study of Cu2ZnSnSe4 bulk crystals. Applied Physics Letters, 2014, 105, 061909.	3.3	26
104	ZnS grain size effects on near-resonant Raman scattering: optical non-destructive grain size estimation. CrystEngComm, 2014, 16, 4120.	2.6	105
105	Two ideal compositions for kesterite-based solar cell devices. , 2014, , .		3
106	Vibrational and structural properties of Cu <inf>2</inf> ZnSn(S <inf>x</inf> Se <inf>1−x</inf>) <inf>4</inf> (0 ≤ x ≤ 1) solid solutions. , 2014, , .		0
107	Discrimination and detection limits of secondary phases in Cu2ZnSnS4 using X-ray diffraction and Raman spectroscopy. Thin Solid Films, 2014, 569, 113-123.	1.8	98
108	Precursor Stack Ordering Effects in Cu ₂ ZnSnSe ₄ Thin Films Prepared by Rapid Thermal Processing. Journal of Physical Chemistry C, 2014, 118, 17291-17298.	3.1	53

#	Article	IF	CITATIONS
109	Earth-abundant absorber based solar cells onto low weight stainless steel substrate. Solar Energy Materials and Solar Cells, 2014, 130, 347-353.	6.2	33
110	Impact of Sn(S,Se) Secondary Phases in Cu ₂ ZnSn(S,Se) ₄ Solar Cells: a Chemical Route for Their Selective Removal and Absorber Surface Passivation. ACS Applied Materials & Interfaces, 2014, 6, 12744-12751.	8.0	132
111	Multiwavelength excitation Raman scattering study of polycrystalline kesterite Cu2ZnSnS4 thin films. Applied Physics Letters, 2014, 104, .	3.3	249
112	Combined Raman scattering/photoluminescence analysis of Cu(In,Ga)Se2 electrodeposited layers. Solar Energy, 2014, 103, 89-95.	6.1	16
113	Optical phonons in the wurtzstanniteCu2ZnGeS4semiconductor: Polarized Raman spectroscopy and first-principle calculations. Physical Review B, 2014, 89, .	3.2	24
114	Pneumatically sprayed Cu ₂ ZnSnS ₄ films under Ar and Ar–H ₂ atmosphere. Journal Physics D: Applied Physics, 2014, 47, 245101.	2.8	17
115	Raman scattering crystalline assessment of polycrystalline Cu2ZnSnS4 thin films for sustainable photovoltaic technologies: Phonon confinement model. Acta Materialia, 2014, 70, 272-280.	7.9	115
116	ZnSe Etching of Znâ€Rich Cu ₂ ZnSnSe ₄ : An Oxidation Route for Improved Solarâ€Cell Efficiency. Chemistry - A European Journal, 2013, 19, 14814-14822.	3.3	118
117	Antimony-Based Ligand Exchange To Promote Crystallization in Spray-Deposited Cu ₂ ZnSnSe ₄ Solar Cells. Journal of the American Chemical Society, 2013, 135, 15982-15985.	13.7	107
118	A thermal route to synthesize photovoltaic grade CuInSe2 films from printed CuO/In2O3 nanoparticle-based inks under Se atmosphere. Journal of Renewable and Sustainable Energy, 2013, 5, 053140.	2.0	4
119	Polarized Raman scattering analysis of Cu ₂ ZnSiS ₄ and Cu ₂ ZnSiSe ₄ single crystals. Journal of Applied Physics, 2013, 114, 173507.	2.5	29
120	Polarized Raman scattering analysis of Cu2ZnSnSe4 and Cu2ZnGeSe4 single crystals. Journal of Applied Physics, 2013, 114, 193514.	2.5	70
121	UV-Raman scattering assessment of ZnO:Al layers from Cu(In, Ga)Se <inf>2</inf> based solar cells: Application for fast on-line process monitoring. , 2013, , .		0
122	Selective detection of secondary phases in Cu <inf>2</inf> ZnSn(S, Se) <inf>4</inf> based absorbers by pre-resonant Raman spectroscopy. , 2013, , .		12
123	Compositional optimization of photovoltaic grade Cu2ZnSnS4 films grown by pneumatic spray pyrolysis. Thin Solid Films, 2013, 535, 67-72.	1.8	66
124	Impact of electronic defects on the Raman spectra from electrodeposited Cu(In,Ca)Se2 solar cells: Application for non-destructive defect assessment. Applied Physics Letters, 2013, 102, .	3.3	30
125	On the formation mechanisms of Zn-rich Cu2ZnSnS4 films prepared by sulfurization of metallic stacks. Solar Energy Materials and Solar Cells, 2013, 112, 97-105.	6.2	200
126	Cu2ZnSnS4 thin films grown by flash evaporation and subsequent annealing in Ar atmosphere. Thin Solid Films, 2013, 535, 62-66.	1.8	20

#	Article	IF	CITATIONS
127	Raman scattering and disorder effect in Cu ₂ ZnSnS ₄ . Physica Status Solidi - Rapid Research Letters, 2013, 7, 258-261.	2.4	136
128	Single‣tep Sulfo‣elenization Method to Synthesize Cu ₂ ZnSn(S _{<i>y</i>} Se _{1â"<i>y</i>}) ₄ Absorbers from Metallic Stack Precursors. ChemPhysChem, 2013, 14, 1836-1843.	2.1	54
129	Secondary phases dependence on composition ratio in sprayed Cu2ZnSnS4 thin films and its impact on the high power conversion efficiency. Solar Energy Materials and Solar Cells, 2013, 117, 246-250.	6.2	116
130	Inhibiting the absorber/Mo-back contact decomposition reaction in Cu2ZnSnSe4 solar cells: the role of a ZnO intermediate nanolayer. Journal of Materials Chemistry A, 2013, 1, 8338.	10.3	151
131	The three A symmetry Raman modes of kesterite in Cu_2ZnSnSe_4. Optics Express, 2013, 21, A695.	3.4	45
132	Preparation of 4.8% efficiency Cu <inf>2</inf> ZnSnSe <inf>4</inf> based solar cell by a two step process. , 2012, , .		2
133	Developing Raman scattering as quality control technique: Correlation with presence of electronic defects in CIGS-based devices. , 2012, , .		1
134	Composition Control and Thermoelectric Properties of Quaternary Chalcogenide Nanocrystals: The Case of Stannite Cu ₂ CdSnSe ₄ . Chemistry of Materials, 2012, 24, 562-570.	6.7	153
135	Vibrational properties of stannite and kesterite type compounds: Raman scattering analysis of Cu2(Fe,Zn)SnS4. Journal of Alloys and Compounds, 2012, 539, 190-194.	5.5	201
136	Design and electrochemical preparation of inductive copper coils for magnetic particles detection. Sensors and Actuators B: Chemical, 2012, 173, 737-744.	7.8	5
137	Raman analysis of monoclinic Cu2SnS3 thin films. Applied Physics Letters, 2012, 100, .	3.3	232
138	Development of a Selective Chemical Etch To Improve the Conversion Efficiency of Zn-Rich Cu ₂ ZnSnS ₄ Solar Cells. Journal of the American Chemical Society, 2012, 134, 8018-8021.	13.7	242
139	Electromagnetic harvester device for scavenging ambient mechanical energy with slow, variable, and randomness nature. , 2011, , .		2
140	Comprehensive Comparison of Various Techniques for the Analysis of Elemental Distributions in Thin Films. Microscopy and Microanalysis, 2011, 17, 728-751.	0.4	72
141	In-depth resolved Raman scattering analysis for the identification of secondary phases: Characterization of Cu2ZnSnS4 layers for solar cell applications. Applied Physics Letters, 2011, 98, .	3.3	287
142	Detection of a ZnSe secondary phase in coevaporated Cu2ZnSnSe4 thin films. Applied Physics Letters, 2011, 98, .	3.3	195
143	Process monitoring of chalcopyrite photovoltaic technologies by Raman spectroscopy: an application to low cost electrodeposition based processes. New Journal of Chemistry, 2011, 35, 453-460.	2.8	52
144	Raman scattering analysis of Cu-poor Cu(In,Ga)Se2 cells fabricated on polyimide substrates: Effect of Na content on microstructure and phase structure. Thin Solid Films, 2011, 519, 7300-7303.	1.8	29

#	Article	IF	CITATIONS
145	Assessment of absorber composition and nanocrystalline phases in CuInS2 based photovoltaic technologies by ex-situ/in-situ resonant Raman scattering measurements. Solar Energy Materials and Solar Cells, 2011, 95, S83-S88.	6.2	27
146	Process monitoring and in line composition assessment of high throughput thin film processes by resonant Raman spectroscopy. , 2011, , .		0
147	Cu deficiency in multi-stage co-evaporated Cu(In,Ga)Se2 for solar cells applications: Microstructure and Ga in-depth alloying. Acta Materialia, 2010, 58, 3468-3476.	7.9	61
148	Advanced diagnostic and control methods of processes and layers in CIGS solar cells and modules. Progress in Photovoltaics: Research and Applications, 2010, 18, 467-480.	8.1	72
149	Influence of NaF incorporation during Cu(In,Ca)Se <inf>2</inf> growth on microstructure and photovoltaic performance. , 2010, , .		15
150	Electrochemical synthesis of CuIn(S,Se)2 alloys with graded composition for high efficiency solar cells. Applied Physics Letters, 2009, 94, 061915.	3.3	20
151	Raman scattering based strategies for quality control and process monitoring in electrodeposited CuIn(S,Se)2 solar cell technologies. Materials Research Society Symposia Proceedings, 2009, 1165, 1.	0.1	Ο
152	Characterisation of Secondary Phases in Cu Poor CuInSe2: Surface and in-depth resolved Raman scattering analysis of polycrystalline layers. Materials Research Society Symposia Proceedings, 2009, 1165, 1.	0.1	2
153	Linear and non-linear behavior of mechanical resonators for optimized inertial electromagnetic microgenerators. Microsystem Technologies, 2009, 15, 1217-1223.	2.0	16
154	Electrodeposition based synthesis of S-rich Culn(S,Se)2 layers for photovoltaic applications: Raman scattering analysis of electrodeposited CulnSe2 precursors. Thin Solid Films, 2009, 517, 2163-2166.	1.8	21
155	Raman scattering and structural analysis of electrodeposited CuInSe ₂ and Sâ€rich quaternary CuIn(S,Se) ₂ semiconductors for solar cells. Physica Status Solidi (A) Applications and Materials Science, 2009, 206, 1001-1004.	1.8	51
156	Analysis of sulphurisation processes of electrodeposited S-rich Culn(S,Se)2 layers for photovoltaic applications. Thin Solid Films, 2009, 517, 2264-2267.	1.8	12
157	Key role of Cu–Se binary phases in electrodeposited CuInSe2 precursors on final distribution of Cu–S phases in CuIn(S,Se)2 absorbers. Thin Solid Films, 2009, 517, 2268-2271.	1.8	29
158	In-depth resolved Raman scattering analysis of secondary phases in Cu-poor CuInSe2 based thin films. Applied Physics Letters, 2009, 95, 121907.	3.3	40
159	Investigation of compositional inhomogeneities in complex polycrystalline Cu(In,Ga)Se2 layers for solar cells. Applied Physics Letters, 2009, 95, .	3.3	43
160	Design and fabrication of Si technology miicrogenerators for vibrational energy scavenging. , 2009, , .		0
161	Raman scattering microcrystalline assessment and device quality control of electrodeposited CuIn(S,Se)2 based solar cells. Thin Solid Films, 2008, 516, 7021-7025.	1.8	12
162	Design and implementation of mechanical resonators for optimized inertial electromagnetic microgenerators. Microsystem Technologies, 2008, 14, 653-658.	2.0	42

#	Article	IF	CITATIONS
163	Raman scattering characterisation of electrochemical growth of CuInSe ₂ nanocrystalline thin films for photovoltaic applications: Surface and inâ€depth analysis. Surface and Interface Analysis, 2008, 40, 798-801.	1.8	31
164	Optimisation of copper electrodeposition processes for Si technology based inductive microsystems. Journal of Electroanalytical Chemistry, 2008, 619-620, 176-182.	3.8	7
165	Analysis of S-rich Culn(S,Se)2 layers for photovoltaic applications: Influence of the sulfurization temperature on the crystalline properties of electrodeposited and sulfurized CulnSe2 precursors. Journal of Applied Physics, 2008, 103, 123109.	2.5	34
166	Linear and non linear behavior of mechanical resonators for optimized inertial electromagnetic microgenerators. , 2008, , .		2
167	Field effect white and tunable electroluminescence from ion beam synthesized Si- and C-rich SiO2 layers. Applied Physics Letters, 2007, 91, 211105.	3.3	15
168	Design and implementation of mechanical resonators for optimized inertial electromagnetic microgenerators. , 2007, , .		1
169	Raman microprobe characterization of electrodeposited S-rich Culn(S,Se)2 for photovoltaic applications: Microstructural analysis. Journal of Applied Physics, 2007, 101, 103517.	2.5	66
170	Electrodeposited CuIn(S, Se)2 films for low cost high efficiency solar cell applications: microstructural analysis. , 2007, , .		1
171	Electroluminescence from C- and Si- rich silicon oxides in continuous wave and pulsed excitation. , 2007, , .		0
172	Microinductive Signal Conditioning With Resonant Differential Filters: High-Sensitivity Biodetection Applications. IEEE Transactions on Instrumentation and Measurement, 2007, 56, 1590-1595.	4.7	9
173	Vibrational energy scavenging with Si technology electromagnetic inertial microgenerators. Microsystem Technologies, 2007, 13, 1655-1661.	2.0	50
174	Si technology based microinductive devices for biodetection applications. Sensors and Actuators A: Physical, 2006, 132, 499-505.	4.1	10
175	Charge transport along luminescent oxide layers containing Si and SiC nanoparticles. Journal of Luminescence, 2006, 121, 356-360.	3.1	5
176	White electroluminescence from C- and Si-rich thin silicon oxides. Applied Physics Letters, 2006, 89, 253124.	3.3	21
177	Electrochemical deposition of Cu and Ni/Cu multilayers in Si Microsystem Technologies. Sensors and Actuators A: Physical, 2005, 123-124, 633-639.	4.1	19
178	Real-time study of phase transformations in Cu–In chalcogenide thin films using in situ Raman spectroscopy and XRD. Journal of Physics and Chemistry of Solids, 2005, 66, 1954-1960.	4.0	27
179	Effect of excess vacancies in ion beam synthesis of SiC nanoclusters. Vacuum, 2005, 78, 177-180.	3.5	3
180	Characterisation and stabilisation of Pt/TaSix/SiO2/SiC gas sensor. Sensors and Actuators B: Chemical, 2005, 109, 119-127.	7.8	10

Alejandro Pérez-RodrÃgue

#	Article	IF	CITATIONS
181	In situ and ex situ characterisation of thermally induced crystallisation of CuInS2 thin films for solar cell. Thin Solid Films, 2005, 480-481, 362-366.	1.8	20
182	Vibrational and crystalline properties of polymorphicCuInC2(C=Se,S)chalcogenides. Physical Review B, 2005, 71, .	3.2	86
183	Time-resolved analysis of the white photoluminescence from SiO2 films after Si and C coimplantation. Applied Physics Letters, 2004, 84, 25-27.	3.3	29
184	Synthesis of nano-sized SiC precipitates in Si by simultaneous dual-beam implantation of C + and Si + ions. Applied Physics A: Materials Science and Processing, 2003, 76, 827-835.	2.3	15
185	Real-time investigations of the influence of sodium on the properties of Cu-poor prepared CuInS2 thin films. Thin Solid Films, 2003, 431-432, 110-115.	1.8	20
186	<title>Raman scattering and microstructural analysis of polycrystalline CuInS2 films for solar cell devices</title> . , 2003, 5024, 117.		1
187	Luminescence and Morphological Properties of GaN Layers Grown on SiC/Si(111) Substrates. Physica Status Solidi A, 2002, 192, 401-406.	1.7	2
188	SiCOI Structures. Technology and Characterization. , 2002, , 17-29.		1
189	Growth and characterization of shape memory alloy thin films for Si microactuator technologies. Journal of Materials Science: Materials in Electronics, 2001, 12, 323-326.	2.2	6
190	Ostwald ripening of Ge precipitates elaborated by ion implantation in SiO2. Materials Science and Engineering B: Solid-State Materials for Advanced Technology, 2000, 69-70, 380-385.	3.5	16
191	Raman spectroscopy and microhardness of ion-implanted a-C:H-films. Ceramics International, 2000, 26, 29-32.	4.8	5
192	An electron microscopy study of the growth of Ge nanoparticles in SiO2. Applied Physics Letters, 2000, 76, 3962-3964.	3.3	46
193	Ion beam synthesis of polycrystalline SiC on SiO2structures for MEMS applications. Journal of Micromechanics and Microengineering, 2000, 10, 152-156.	2.6	9
194	Optical Spectroscopy of SOI Materials. , 2000, , 137-148.		0
195	Test microstructures for measurement of SiC thin film mechanical properties. Journal of Micromechanics and Microengineering, 1999, 9, 190-193.	2.6	13
196	Measurement of micromechanical properties of polysilicon microstructures with an atomic force microscope. Sensors and Actuators A: Physical, 1998, 67, 215-219.	4.1	42
197	Physical techniques for silicon layer analysis. Microelectronic Engineering, 1998, 40, 223-237.	2.4	19
198	Diagnostics of nitrogen-implanted diamond-like carbon films by optical and microhardness		0

measurements. , 1998, 3359, 339.

#	Article	IF	CITATIONS
199	Optical characterization of carbon ion implantation into Si and SiGe alloys. , 1998, 3359, 324.		0
200	Analysis of ion beam induced damage and amorphization of 6H-SiC by raman scattering. Journal of Electronic Materials, 1996, 25, 541-547.	2.2	66
201	Detailed analysis of β-SiC formation by high dose carbon ion implantation in silicon. Materials Science and Engineering B: Solid-State Materials for Advanced Technology, 1996, 36, 282-285.	3.5	17
202	Synthesis of Thin Membranes in Si Technology by Carbon Ion Implantation. Materials Research Society Symposia Proceedings, 1995, 396, 727.	0.1	1
203	Ion beam synthesis of aluminium nitride: characterisation of thin AIN layers formed in microelectronics aluminium. Materials Science and Technology, 1995, 11, 1187-1190.	1.6	2
204	The characteristics of intimate Auî—,InyAl1 â^' yAs Schottky diodes: a mismatch dependence study. Materials Science and Engineering B: Solid-State Materials for Advanced Technology, 1994, 28, 433-438.	3.5	0
205	Anisotropic etch-stop properties of nitrogen-implanted silicon. Sensors and Actuators A: Physical, 1994, 45, 219-225.	4.1	4
206	Non-destructive characterization of the uniformity of thin cobalt disilicide films by Raman microprobe measurements. Thin Solid Films, 1994, 251, 45-50.	1.8	16
207	Structural analysis of buried AlN thin films formed by nitrogen implantation into microelectronics grade aluminium. Nuclear Instruments & Methods in Physics Research B, 1994, 84, 214-217.	1.4	7
208	Optical characterisation of SIMOX structures formed by successive implantation and annealing. Nuclear Instruments & Methods in Physics Research B, 1994, 84, 275-280.	1.4	3
209	Infrared analysis of buried insulator layers formed by ion implantation into silicon. Applied Surface Science, 1993, 63, 312-315.	6.1	4
210	Buried oxide layers formed by oxygen implantation on screened oxide silicon wafers: structural analysis. Nuclear Instruments & Methods in Physics Research B, 1993, 80-81, 838-841.	1.4	3
211	Analysis of the SiO2 defects originated by phosphorus implantation in MOS structures. Nuclear Instruments & Methods in Physics Research B, 1993, 80-81, 612-615.	1.4	1
212	Structural characterisation of nitrogen ion implantation into silicon for sensor technology. Nuclear Instruments & Methods in Physics Research B, 1993, 80-81, 702-705.	1.4	3
213	Analysis of buried etch-stop layers in silicon by nitrogen-ion implantation. Journal of Micromechanics and Microengineering, 1993, 3, 143-145.	2.6	160
214	Effects of electric field on photoconductive frequency resolved spectroscopy: Analysis of silicon-on-insulator structures. Solid-State Electronics, 1992, 35, 1337-1342.	1.4	0
215	Design of a microinductive device integrated within a simple resonant diferential filter for high sensitivity portable biodetectors. , 0, , .		0
216	Electrical response of MOSiC gas sensors to CO, NO/sub 2/ and C/sub 3/H/sub 8/. , 0, , .		0

#	Article	IF	CITATIONS
217	Microcoils for biosensors fabricated by focused ion beam (FIB). , 0, , .		2
218	Thickness evaluation of AlO x barrier layers for encapsulation of flexible PV modules in industrial environments by normal reflectance and machine learning. Progress in Photovoltaics: Research and Applications, 0, , .	8.1	2
219	Thin Film Sb2(S,Se)3 Based Solar Cell: Emergent Technology Compatible with Ubiquitous Applications. , 0, , .		0
220	Thin Film Sb2(S,Se)3 Based Solar Cell: Emergent Technology Compatible with Ubiquitous Applications. , 0, , .		0